Chemistry - Methods

Chemistry—Methods

Chemistry Europe
European Chemical Societies Publishing

RESEARCH ARTICLE OPEN ACCESS

Mechanochemically Driven Synthesis of Anticancer Cocrystals: A Case Study of Lenalidomide

Ana C. S. Carvalho[1,2] | M. Teresa Duarte[1] | Clara S. B. Gomes[3] | Mafalda Sarraguça[4] | Alessia Bacchi[5,6] | Michele Prencipe[5] | Job Gieling[7] | Natalia Shemchuk[7] | Daniel M. Baier[7] | Koen Robeyns[7] | Hector Polyzois[8] | Lidia Tajber[8] | Christos M. Chatzigiannis[9] | Evelina Colacino[9] | Tom Leyssens[7] | Vânia André[1,2]

[1]Centro de Química Estrutural, Institute of Molecular Sciences, Instituto Superior Técnico, Universidade de Lisboa, Lisbon, Portugal | [2]Associação do Instituto Superior Técnico para a Investigação e Desenvolvimento (IST-ID), Lisbon, Portugal | [3]LAQV-REQUIMTE, NOVA School of Science and Technology (NOVA FCT), NOVA University of Lisbon, Caparica, Portugal | [4]LAQV, REQUIMTE, Faculdade de Farmácia, Universidade do Porto, Porto, Portugal | [5]Consorzio Interuniversitario per lo sviluppo dei Sistemi a Grande Interfase, Sesto Fiorentino (FI), Italy | [6]Dipartimento di Scienze Chimiche, della Vita, e della Sostenibilità Ambientale, Università di Parma, Parma, Italy | [7]Department of Molecular Chemistry, Materials and Catalysis, Institute of Condensed Matter and Nanosciences, Louvain-La-Neuve, Belgium | [8]School of Pharmacy and Pharmaceutical Sciences, Trinity College Dublin, Dublin, Ireland | [9]ICGM, Univ Montpellier, CNRS, ENSCM, France

Correspondence: Tom Leyssens (tom.leyssens@uclouvain.be) | Vânia André (vaniandre@tecnico.ulisboa.pt)

Received: 7 January 2026 | **Revised:** 26 February 2026 | **Accepted:** 28 February 2026

Keywords: flavonoids | lenalidomide | liquid-assisted grinding (LAG) | mechanochemistry | pharmaceutical cocrystal | resonant acoustic mixing | solubility profile

ABSTRACT

The modulation of physicochemical properties through the discovery of new solid forms has attracted significant interest in the pharmaceutical industry. Herein, a novel cocrystal of lenalidomide with quercetin was designed upon crystal engineering principles. Bearing in mind the importance of developing sustainable methods for the pharmaceutical industry, the synthesis of the novel cocrystals was explored by different mechanochemical approaches and slurry techniques for comparison purposes. Thus, the cocrystal was produced by liquid-assisted grinding in ball milling, liquid-assisted resonant acoustic mixing, and the slurry method. All the methods yielded the same final form with similar properties. From the point of view of properties enhancement, solubility studies showed that the cocrystal exhibited lower solubility than that of pure lenalidomide under simulated conditions of gastric and intestinal fluids, suggesting that the cocrystal may function as an extended-release form of lenalidomide. Furthermore, this cocrystal remained stable under accelerated stability conditions, indicating that atmospheric relative humidity does not represent a risk for the handling or storage of these compounds in the solid state.

1 | Introduction

Recognized by the International Union of Pure and Applied Chemistry (IUPAC) as one of the 10 Emerging Technologies in Chemistry [1], mechanochemistry is a green alternative route for chemical transformations, offering a rapid platform for screening new molecules and materials [2]. In this methodology, chemical reactions are driven by mechanical forces [3, 4], using different methods of activation, scales, and output [1, 3, 5], and are implemented through different devices such as ball mills [1], twin screw extrusion [5], and resonant acoustic mixing (RAM) [6]. A key feature of these reactions is that they can proceed without any solvents (neat grinding, NG), which confers clear advantages over the classical solution chemistry [7]. In contrast, the deliberate addition of a small amount of a catalytic phase during the mechanochemical process can exert significantly enhance reaction efficiency. This catalytic effect can be obtained by the addition of a liquid (liquid-assisted grinding - LAG) [2, 8–11], a liquid and an ionic salt (ion and liquid-assisted grinding) [12], or the addition of a polymer (polymer-assisted grinding) [13]. Due to the efficiency of mechanochemical synthesis, this method has been widely used in the crystal engineering field

for the development of new pharmaceutical materials, enabling the manipulation of supramolecular assemblies by mechanical force [10, 14].

Crystal engineering encompasses the understanding of intermolecular interactions within crystal packing [15, 16], enabling the design of materials with optimized properties [15–19]. Introduced by Pepinsky in 1955 [20] and later popularized by Schmidt [21], this strategy is widely used in the pharmaceutical field, particularly for the development of new solid forms, such as salts, cocrystals, polymorphs, and others aimed at improving physicochemical properties [22, 23]. Currently, the design of cocrystals is a central focus of crystal engineering owing to its efficiency in modulating critical physicochemical properties such as aqueous solubility, stability, permeability, pharmacokinetics, and bioavailability of a drug [17, 18, 22–28].

Cocrystals are "solids that are crystalline single-phase materials composed of two or more different molecular and/or ionic compounds generally in a stoichiometric ratio which are neither solvates nor simple salts" [29]. Typically, a pharmaceutical cocrystal is formed by an active pharmaceutical ingredient (API) and a generally regarded as safe coformer connected by noncovalent intermolecular interactions, such as hydrogen bonds, π–π stacking, halogen bonds, and van der Waals forces, forming supramolecular synthons [30, 31]. Introduced by Desiraju in 1995 [32], supramolecular synthons are structural units typically formed by complementary hydrogen bonds. They arise either from the self-recognition of identical functional groups, referred to supramolecular homosynthons, or from interactions between different but complementary functional groups, forming supramolecular heterosynthons [30, 33, 34]. The design of cocrystals can be achieved mainly by the exploitation of supramolecular synthons, typically based upon complementary hydrogen bonding and hydrogen bond propensity. This approach enables a rational design strategy by estimating the probability of a specific intermolecular interaction between the API and the coformer, thus indicating the potential for cocrystal formation [35–37]. The likelihood of competing homosynthons and target heterosynthons for cocrystal formation can be achieved by data mining using the Cambridge Structural Database (CSD) [38]. This approach results in a shortlist of coformer molecules presenting the preferred hydrogen bond synthons and offers a useful guide for the rational design of multicomponent cocrystals [18, 35].

These multicomponent crystals can be prepared by different methods such as solution crystallization, including antisolvent addition, slow evaporation and cooling crystallization, slurry, hot melt extrusion, sonochemical, mechanochemical synthesis, and others [18, 39–42]. Among these methods, mechanochemistry has gained particular prominence in the scientific community due to its efficiency in screening, discovery, and scale-up of cocrystal forms [43, 44]. Combining mechanochemistry with crystal engineering strategies can lead to valuable insights into the mechanisms of mechanochemical reactions involving noncovalent bonds [14].

The ability of cocrystals to modify the physicochemical properties of a drug without changing its molecular structure may simplify the drug development process and regulatory approval as the drug remains the same [18]. As the drug solubility directly impacts bioavailability and absorption levels, and consequently drug efficacy and safety, its optimization plays a key role in overall therapeutic performance [45]. Depending on the specific components and conditions, cocrystals may either increase or decrease the solubility of a compound, modulating its therapeutic effect [46].

Lenalidomide (LENA, $C_{13}H_{13}N_3O_3$) is a 4-amino-glutarimide analogue of thalidomide [47], that works as an immunomodulatory agent with antiangiogenic and antineoplastic properties [30]. LENA has been used in the treatment for multiple myeloma and for transfusion-dependent anaemia caused by myelodysplastic syndromes [30, 47, 48]. Lenalidomide hemihydrate is the API present in Revlimid.

A CSD [38] survey shows that there are two polymorphs of anhydrous LENA [49, 50], five hydrates [48–51], three solvates [50], three anhydrous cocrystals [30, 48], one hydrated cocrystal [30], one solvate hemihydrate cocrystal [46], and three hydrated salts [52, 53]. Solubility studies were reported for several of these forms. LENA•3,5-dihydroxybenzoic acid cocrystal [30] presented an improvement in the solubility, but a "spring and parachute effect" was observed [30]. The LENA•gallic acid cocrystal also showed higher solubility and a better dissolution profile than LENA, but, in this case, the "spring and parachute effect" was not observed [48]. In contrast, the LENA•melamine cocrystal has lower aqueous solubility than pure LENA [46].

A final form with lower solubility is often advantageous for systems in which extended drug release is beneficial. For example, due to lower and flatter drug dissolution profiles in the lungs, these lower soluble cocrystals can be useful for pulmonary drug delivery, benefiting from the reduced frequency of doses that a patient is required to take [54]. LENA is rapidly absorbed following oral administration and has the potential for acute toxicity; thus, a less frequent administration regime has been suggested for this drug [55]. In this context, a formulation of LENA that produces lower plasma concentration peaks may offer improved safety and therapeutic benefit for patients. Interestingly, from the synthesis point of view, a combination of mechanochemical followed by slurry method was applied to obtain the abovementioned LENA cocrystals [30, 48].

In addition to the CSD survey, further studies including molecular complementarity and hydrogen bonds propensities were conducted for the cocrystal design [37], revealing a tendency for interaction of anhydrous LENA (CSD Ref.code AJISES) with amino acids, carboxylic acids, and phenolic derivatives. Among these compounds, flavonoids, a class of natural polyphenolic compounds, have received great attention in the scientific community, mainly because they can act as coadjuvants in treating a wide range of diseases, including cancer, cardiovascular diseases, and immunological disorders [56–61]. In addition, various authors have reported a synergistic effect when flavonoids are employed as cocrystal formers with APIs in cancer treatment [62–66].

Belonging the list of generally recognized as safe compounds [67], quercetin (QUER), a polyphenolic flavonoid nutraceutical widely found in fruits and vegetables, is a potent antioxidative compound, also recognized by the potential therapeutic activity as anticarcinogenic, anti-inflammatory, antiviral, and cardioprotective effects [68]. Quercetin:nutraceutical cocrystals showed an improvement in the antioxidant activity and selective anticancer effects [69]. The incorporation of QUER into a cocrystal would tune a potential synergistic effect when combined with other drugs [68, 70–72], such as LENA. In addition, a novel drug

delivery system (DDS) based on a metal-organic framework modified with quercetin and loaded with a lenalidomide derivative (L1) has been reported [73]. The results showed that the incorporation of QUER in this DDS increases significantly the activity against the triple negative breast cancer cell lines [73], highlighting the potential synergistic effect of QUER.

Although QUER has been widely recognized for its potential to form cocrystals with antitumoral activity, and several studies report the preparation of LENA cocrystals, the LENA•QUER cocrystal system reported herein is the first example of a polyphenolic flavonoid nutraceutical compound (QUER) combined with LENA. This cocrystal was explored via LAG by ball milling and liquid-assisted resonant acoustic mixing (LA-RAM), emphasizing the efficiency and sustainability of these approaches compared to solvent-based crystallization methods. In this context, this work presents a comprehensive structural, physicochemical, solid state, and solubility characterization of the novel cocrystal, offering a strategy to modulate LENA solubility. Furthermore, the stability of the cocrystal under accelerated conditions was evaluated, confirming its suitability for handling and storage. This study brings new insights to potentially achieve a synergistic effect when using the two molecules.

2 | Results and Discussion

2.1 | Cocrystal Design

In this work, crystal engineering strategies were applied in the design of new cocrystals [74]. A virtual cocrystal screening applying molecular complementarity and hydrogen-bond propensity was carried out, and a family of 62 coformers containing simultaneously carboxylic acids and amine moieties was reached.

The potential landscape of supramolecular contacts was inspected by using the Full Interaction Map tool of the CSD software suite, which allows the identification and visualization of a molecular region with a propensity to form specific intermolecular interactions, based on experimental crystallographic data. The software generates three-dimensional maps that highlight the likelihood of hydrogen, halogen, or π-π contacts, facilitating the quantitative analysis of noncovalent interactions. It is particularly useful in cocrystal design, drug design, and in the study of molecular complementarity. The full LENA's interaction map computed on Mercury (2023.1) shows that the interactions are not univocal nor optimally distributed, while QUER shows that some interactions could be replaced in other arrangements: in Figure 1a, the arrows highlight two areas with high propensity to accept hydrogen bonds with NH/OH donors (blue and red regions), which are not matched by the actual contacts found in the experimental LENA crystal structure (red balls, representing O donors/acceptors in the structure). This implies that the crystal packing of LENA is not optimally realizing all the potential interactions. Similarly, for QUER (Figure 1b), the two blue areas indicated by arrows are regions where, according to the screening of experimental crystal structures of similar compounds in the CSD, one would expect to find a hydrogen bond donor, while in the actual QUER structure there are no interactions matching those potential interaction sites. This analysis suggests that the combination of the two molecules could better respond to the optimization of supramolecular interactions [75].

2.2 | Methods for Cocrystal Preparation

This study aimed to evaluate two alternative mechanochemical routes—LAG via ball milling and LA-RAM—for producing the LENA•QUER cocrystal, in comparison with slurry- and solution-based methods. An extensive screening of synthetic methodologies, ranging from mechanochemical to solution-based approaches, was conducted to obtain the LENA•QUER cocrystal. Four successful protocols for its synthesis are presented (Scheme 1). A detailed description of the synthetic procedures and characterization techniques is presented in the Experimental Section of Supporting Information. Comparing the previously reported synthesis for other LENA cocrystals [30, 46, 48], the procedures presented herein offer the advantage of being one-pot reactions, requiring no further purification.

It is well established that for mechanochemical processes several parameters, such as milling frequency, milling time, milling media, additives, and temperature (among others), can directly affect the selectivity and yield of a mechanochemical reaction [1], by subtly modulating noncovalent bonding [14]. In this context, a screening for the LENA•QUER cocrystal was conducted by ball-milling experiments in 10 mL stainless steel (SS) jars using two SS ball-milling media (Ø = 7 mm). Milling frequency, synthesis time, solvent type (including ethanol, methanol, acetonitrile, ethyl acetate, and water), and solvent quantity were the most important parameters tested (Table S1, Supporting Information).

The addition of a liquid additive during milling reactions, measured by the ratio of liquid volume to reactant weight (η), is a

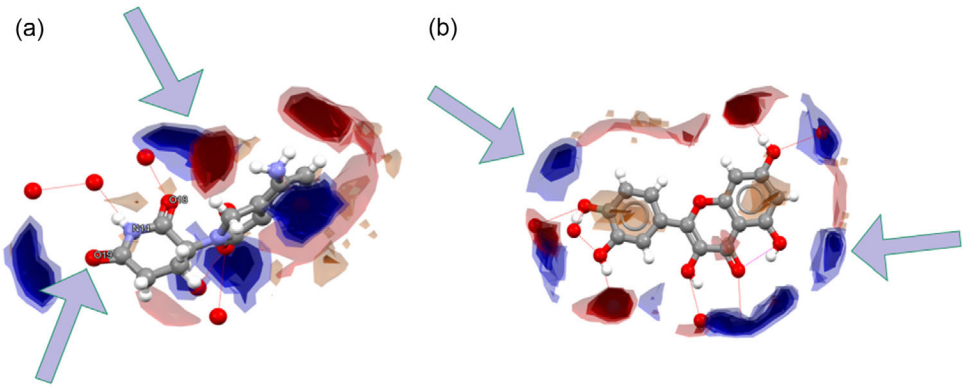

FIGURE 1 | The full interaction maps (Mercury) of (a) LENA and (b) QUER.

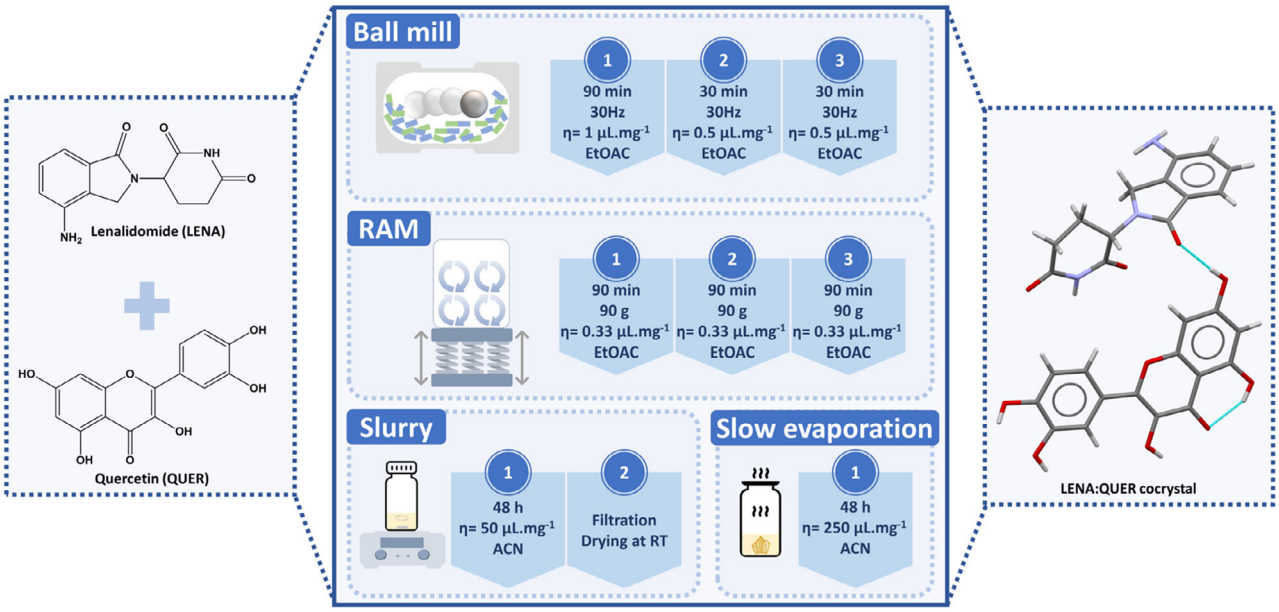

SCHEME 1 | Optimized approaches to obtain LENA•QUER cocrystal.

critical parameter to be adjusted. Beyond the catalytic effect [5], the nature of this additive can also lead to polymorphic control [76]. In the presence of water, both LENA and QUER converted into hydrated forms, hindering the formation of cocrystals (Figure S1, Supporting Information). Furthermore, when compounds were milled with ethanol (EtOH), QUER transformed into a new crystalline form, and no cocrystal formation was observed (Figure S2, Supporting Information).

As the frequency can directly affect the number of collisions during a milling process [1], selecting a higher milling frequency was crucial to induce the formation of the cocrystal between LENA and QUER, leading to a complete conversion.

A successful BM synthetic approach was obtained in a one-pot reaction involving three steps of liquid addition followed by milling. In the first step, ethyl acetate (EtOAC, $\eta = 1\ \mu L.mg^{-1}$) was added to a 1:1 molar ratio of the reactants and milled for 90 min at 30 Hz, resulting in incomplete conversion. Subsequently, two more milling steps were conducted by adding again EtOAC ($\eta = 0.5\ \mu L.mg^{-1}$) in each of these two steps and milling for additional 30 min at 30 Hz in each step. This procedure led to complete conversion into the LENA•QUER cocrystal (Figure 2a). Attempts to obtain the cocrystal in a single step, by combining the total time and amount of solvent as used in the three-steps synthesis, always resulted in incomplete reactions. These results indicate that the optimized procedure by LAG using a ball mill requires successive addition of EtOAC followed by milling.

The formation of LENA•QUER cocrystal was also systematically investigated at 90 g by RAM in liquid-assisted mixing (LA-RAM), in continuous or by cycles of mixing. Comprehensive screening of various experimental conditions included the nature of the solvent for LA-RAM (acetonitrile, EtOH, EtOAc, or isopropyl acetate-iPrOAc) and its amount (expressed as η value), the polymeric material used for the reaction vessels (polypropylene, PP or polytetrafluoroethylene, PTFE), and the molar ratio of LENA to

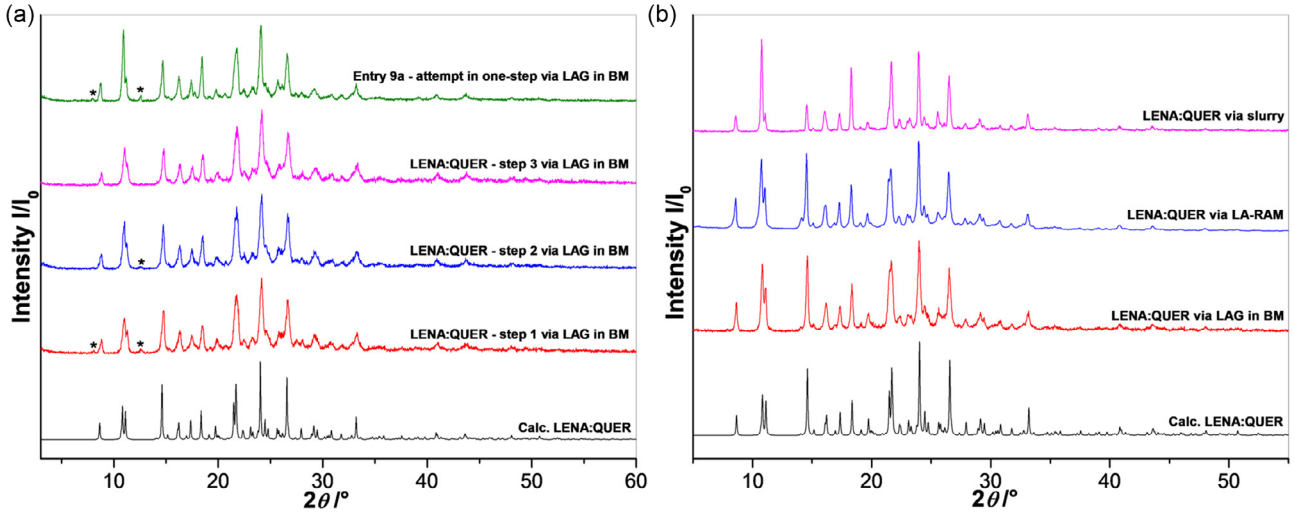

FIGURE 2 | (a) Calculated and experimental PXRD patterns of reaction steps of LENA•QUER cocrystal via ball milling. (b) Calculated and experimental PXRD patterns LENA•QUER cocrystal synthesized by ball milling (BM) in LAG process, LA-RAM, and slurry.

QUER (Table S2, Supporting Information). Initial experiments included a 1:1 molar ratio of the reactants, examining both dry mixing and LA-RAM approaches.

For LA-RAM investigation, EtOH, acetonitrile, and EtOAc were selected as solvents based on their favourable physical properties and safety profiles, using an η value of 0.2 $\mu L.mg^{-1}$. Initial screening conditions of 30 min mixing time, 90 g acceleration, and 2.5 mL PP vials were maintained throughout this series. Notably, solvent selection significantly influenced cocrystal formation, with the reported cocrystal formation being observed exclusively with EtOAc (Table S2, Entries 2–4, Supporting Information).

Further optimization of the η value for ethyl acetate (0.5–1.0 $\mu L.mg^{-1}$) demonstrated improved system rheology and enhanced mixing homogeneity at $\eta = 1.0\ \mu L.mg^{-1}$ (Table S2, Entries 5–7, Supporting Information). Subsequently, extending the mixing time to 90 min enhanced cocrystal formation but failed to achieve complete conversion (Table S2, Entry 8, Supporting Information).

By adopting a stepwise approach analogous to ball-milling methodology, two-step addition of EtOAc over 90 min resulted in complete quercetin conversion, though some unreacted lenalidomide remained (Table S2, Entry 9, Supporting Information). To account for differences in starting material purity, the stoichiometric ratio was adjusted to 1:1.05 (LENA•QUER), achieving complete conversion but generating an unidentified peak at $2\theta = 12.3694°$ that did not correspond to the calculated cocrystal structure (Table S2, Entry 11, Figure S3, Supporting Information).

Additional parameters were systematically evaluated to obtain the pure cocrystal, including isopropyl acetateAcO^{i}Pr as an alternative solvent, different vial materials and volumes, and extended 180-minute reaction times (Table S2, Entries 12–16, Supporting Information). However, these modifications failed to eliminate the problematic peak at $2\theta = 12.3694°$, and in some cases, resulted in incomplete conversion. Ultimately, implementing a three-step mixing protocol of 90 min each at 90 g successfully yielded the desired cocrystal by LA-RAM (Table S2, Entry 17, Supporting Information).

Solution-based experiments were conducted by slow evaporation and slurry, using acetonitrile as a solvent to achieve the cocrystal, and both approaches were successful. In addition, a suitable single crystal was obtained by slow evaporation, allowing the crystal structure elucidation and obtention of calculated powder X-ray diffraction (PXRD). The experimental PXRD patterns of the cocrystal synthesized by ball milling, LA-RAM, and slurry agree with the calculated PXRD patterns obtained by single crystal X-ray diffraction (SCXRD) data (Figure 2b).

Comparing all methodologies developed for the obtention of LENA•QUER cocrystal, the mechanochemical approaches present the advantages of being faster and requiring a lower amount of solvent in the synthetic process in comparison with solution-based methods.

2.3 | Crystal Structure and Supramolecular Analysis

The structure of the LENA•QUER cocrystal disclosed in this study will be compared with the crystal structures of both anhydrous lenalidomide polymorphs (CSD ref.codes AJISES and AJISES01). The crystallographic data of the cocrystal are summarized in Table S3.

In polymorph AJISES, which crystallizes in the $P\bar{1}$ space group and comprises one molecule in the asymmetric unit, the LENA molecule establishes intermolecular interactions forming a centrosymmetric dimeric aggregate by N–H…N hydrogen bonds ($d_{N\cdots N} = 3.260(3)$ Å, ∠N–H…N = 128(4)°) along the *a* axis, generating a $R_2^2(4)$ motif, as previously reported [49]. A self-complementary pyridinedione ring forms centrosymmetric dimers through a $R_2^2(8)$ motif based on N–H…O hydrogen bonds ($d_{N\cdots O} = 2.8987(16)$ Å, ∠N–H…O = 179(2)°) and infinite $C_1^1(11)$ chains along to the *c* axis based on N–H…O interactions ($d_{N\cdots O} = 3.180(2)$ Å, ∠N-H…O = 142(3)°) (Figure S4 and Table S4, Supporting Information).

The other LENA polymorph (CSD Ref. code AJISES01) crystallizes in the *Pbca* space group. In AJISES01, LENA establishes intermolecular interactions $C_1^1(7)$ chains along to the *b* axis based on N–H…O interactions ($d_{N\cdots O} = 2.8043(17)$ Å, ∠N-H…$C_1^1(9)$ chains along the *a* axis based on N–H…O interactions ($d_{N\cdots O} = 3.027(2)$ Å, ∠N-H…O = 162.9(17)°) and a $R_2^2(22)$ motif based on N-H…O hydrogen bonds ($d_{N\cdots O} = 3.067(2)$ Å, ∠N-H…O = 161.5(18)°) (Figure S5 and Table S5, Supporting Information).

Similarly to AJISES, the cocrystal crystallizes in the $P\bar{1}$ space group and comprises one molecule in the asymmetric unit (Figure 3a). All self-complementarity motifs observed in the LENA crystal packing were broken in the LENA•QUER cocrystal formation, giving rise to a new pattern of hydrogen bonds (Figure 3b and Table S6, Supporting Information). In the cocrystal system, LENA entities do not establish any direct hydrogen bonds among themselves, and this behaviour was not observed in the reported cocrystals [30]. Nevertheless, a new $C_1^1(12)$ motif based on O–H…O interactions ($d_{O\cdots O} = 2.848(2)$ Å, ∠O–H…O = 129°) holds the QUER molecules forming an infinite chain along the *c* axis (Figure S6, Supporting Information). This chain pattern was not observed in any of the polymorphs of pure quercetin (CSD Ref.codes: NAFZEC, NAFZEC01, and NAFZEC02).

The LENA•QUER cocrystal structure is stabilized by $O–H_{QUER}\cdots O_{LENA}$ hydrogen bonds ($d_{N\cdots O} = 2.698(3)$ Å, ∠O-H…O = 171(3) °), forming a $D_1^1(2)$ motif between LENA and QUER moieties. In addition, the hydroxyl group from the coformer interacts directly with LENA through $O–H_{QUER}\cdots N_{LENA}$ / $N–H_{LENA}\cdots O_{QUER}$ hydrogen bond forming weak $D_1^1(2)$ motifs based on N–H…O, O–H…O and O–H…N interactions. Furthermore, as observed in other LENA cocrystals [30, 53], weak π–π interactions were observed in the crystal packing along the c axis between the centroids of LENA moieties with the centroid…centroid distance of 3.789(2) Å, and between QUER moieties with the centroid…centroid distance of 4.094(16) Å (Figure 3c). In addition, several motifs with two symmetry independent hydrogen bonds that compose the pattern were also observed in the cocrystal, and some of them are shown in Figure S7, Supporting Information.

2.4 | Hirshfeld Surfaces Analysis

The Hirshfeld surfaces (HS) and the corresponding two-dimensional fingerprint plots were used to complement the study of the packing interactions (Figure 4) [77]. The HS is represented by a colour code, in which the red, white, and blue spots denote,

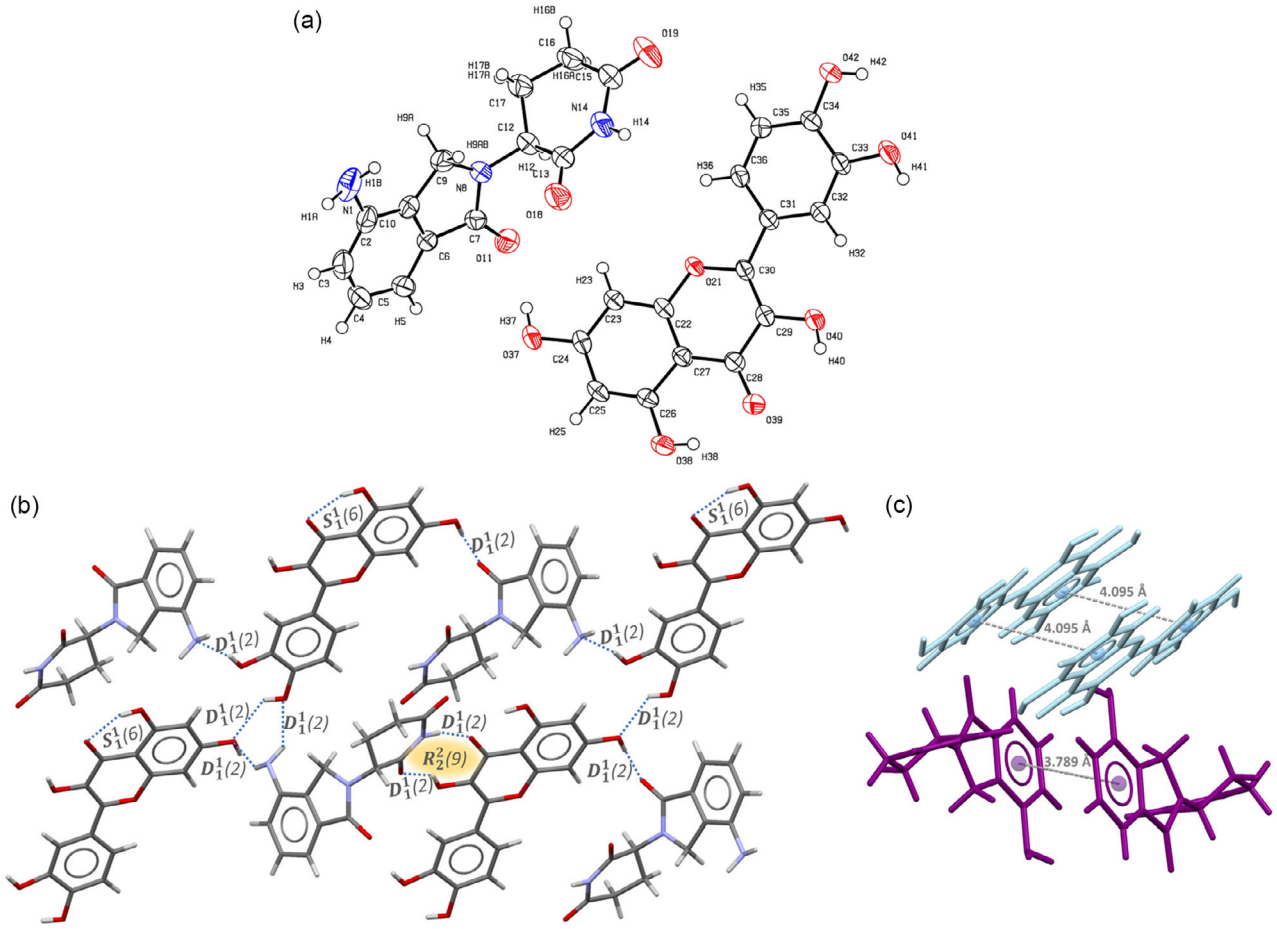

FIGURE 3 | (a) ORTEP projection of LENA•QUER cocrystal with the atom-numbering scheme. Nonhydrogen atoms are represented as 50% probability ellipsoids. Hydrogen bonds are represented by dashed light blue line, (b) 2D layers of LENA•QUER cocrystal, (c) The π…π interactions (grey lines) involved in the stacking arrangement between LENA (purple) and QUER (blue).

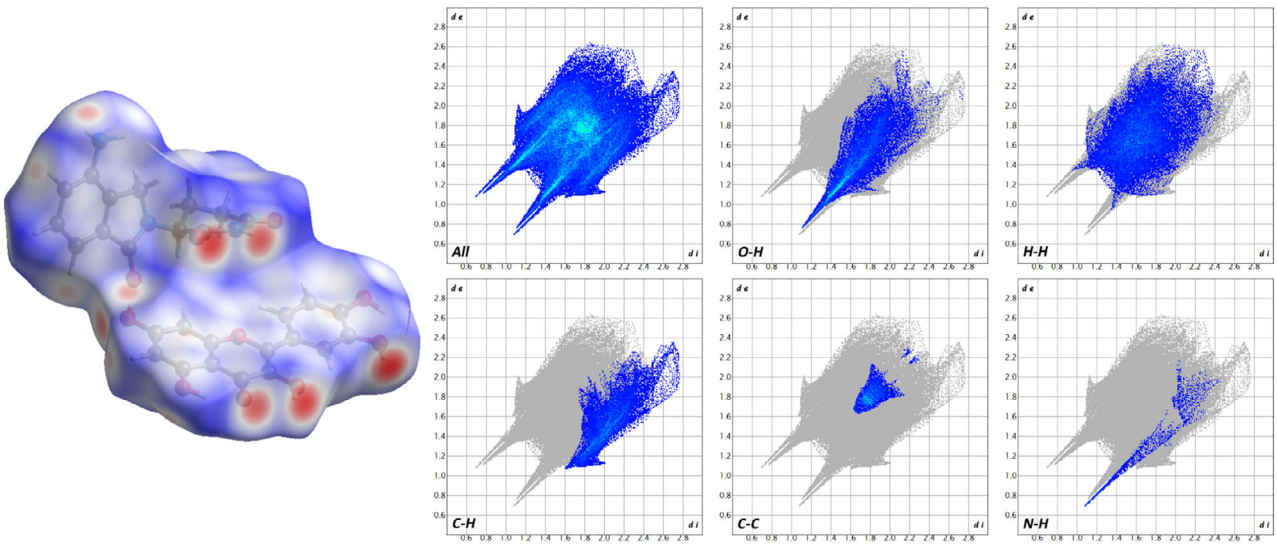

FIGURE 4 | HS mapped with *dnorm* (left) and 2D fingerprint plots (right).

respectively, the intermolecular interactions associated with lengths fewer than, equivalent to, and greater than van der Waal radii [78]. In the fingerprint plots, the d_i represents the distance from HS to the nearest atom internal to the surface, d_e corresponds to the distance from HS to the nearest atom external to the surface, while d_{norm} represents the normalized sum of d_e and d_i [77, 78]. The HS of the LENA•QUER cocrystal has 605.70 Å^3; of volume and 510.54 Å^2; of area. According to the 2D fingerprint

schemes, the O…H and H…H interactions are the most abundant in the cocrystal structure (18.2% and 26.8%, respectively), and these results are in agreement with the supramolecular synthon analysis. The C…H and C…C interactions are also representative (14.0% and 4.6%, respectively), confirming the presence of π–π interactions between adjacent moieties. The N…H interaction does not play a significant role in the crystal structure (1.4%). All other interactions present in minor percentages are detailed in Figure S8, Supporting Information.

2.5 | Attenuated Total Reflectance - Fourier Transform Infrared (ATR-FTIR) Analysis

The ATR-FTIR analyses were carried out for LENA, QUER, and the LENA•QUER cocrystal (Figure 5). LENA presents a typical N-H_{amide} stretch band at 3368 cm^{-1} and 3290 cm^{-1}, a broad band corresponding to the C–$H_{aromatic}$ stretch at 3152 cm^{-1}, and others bands at 1622 cm^{-1}, 1550 cm^{-1}, 1168 cm^{-1} and 1062 cm^{-1} corresponding, respectively, to the $\nu C{=}O_{amide}$, δ N–H_{amine}, δ C–N_{amine}, νC–N_{amine} [79, 80].

Quercetin shows a typical O–H band at 3402 cm^{-1}, a =C–H stretch at 3050 cm^{-1}, C=O stretch at 1714 cm^{-1}, C–O stretch at 1380 cm^{-1}, C–O_{phenol} stretch at 1256 cm^{-1}, and =C–H bending at 896 cm^{-1} [80].

Comparing the LENA•QUER cocrystal with the starting materials, bathochromic displacements of O–H_{phenol} stretch (3484 cm^{-1}) and $C{=}O_{amide}$ stretch (1646 cm^{-1}) are observed, indicating the interaction between LENA and QUER through $C{=}O_{amide}$ from LENA with O–H_{phenol} from QUER. These results agree with supramolecular synthon analysis.

2.6 | Thermal Analysis

The TGA and DSC analysis of both precursors (LENA, QUER) and the LENA•QUER cocrystal are shown in Figure 6.

The thermal decomposition of LENA•QUER occurs in five consecutive steps up to 600°C (details in Figure S9, Supporting Information), in which the first (mass loss of 0.53%) and second (mass loss of 2.53%) steps were attributed to loss of residual solvents adsorbed at the surface (30°C–88°C) with total of 3.06% of weight loss. In the third step (88°C-285°C), a gradual weight loss of 18.29% is observed until the incongruent melting of LENA•QUER cocrystal, which corresponds to the endothermic event at 256°C in the DSC measurement (Figure 6b). The melting is immediately followed by decomposition with the last steps (285–600°C) in the TGA curve corresponding to the thermal decomposition of the two coformers, as confirmed by the TGA curves of the pure components (Figure 6a, S10, and S11, Supporting Information).

Considering the DSC curves (Figure 6b), the endothermic events are attributed to the melting of the compounds, which occur at 269°C (ΔH = −129 J/g) for LENA, and 322°C (ΔH = −143 J/g) for QUER, and 256°C (ΔH = - 119.5 J/g) for the LENA•QUER cocrystal. It is worth noting that the low-intensity endothermic event (100°C–120°C) in the DSC thermogram of QUER may refer to the loss of residual water content, which is supported by a weight loss of 2.24% between 30°C and 115°C (see Figure S11, Supporting Information). As observed in other LENA cocrystals [79], the melting point of the LENA•QUER cocrystal is lower than that of both constituents. This can either reflect an entropy-driven cocrystal formation (with less strong bonding in the cocrystal compared to the parent compounds) or due to a strong entropic mixing effect at the liquid state upon melting of the cocrystal.

It is worth noting that the overall weight loss (decomposition), at 600°C, for the LENA•QUER cocrystal (44.05%) is lower than pure LENA (60.64%) and QUER (67.01%). DSC analysis also showed that the cocrystal presents a lower melting point than the starting materials.

2.7 | Nuclear Magnetic Resonance

The ^{1}H-NMR spectrum of the LENA•QUER cocrystal is shown in Figure 7. Based on the ^{1}H-NMR spectra of the individual

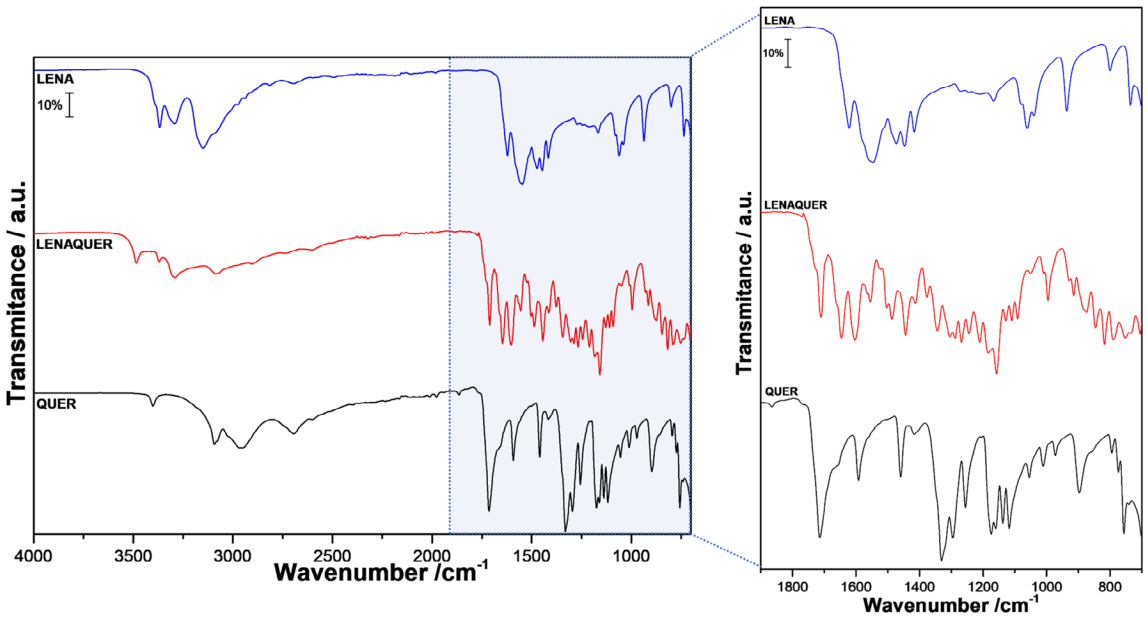

FIGURE 5 | FTIR spectra of LENA (blue), cocrystal (red), and QUER (black) with amplified fingerprint region.

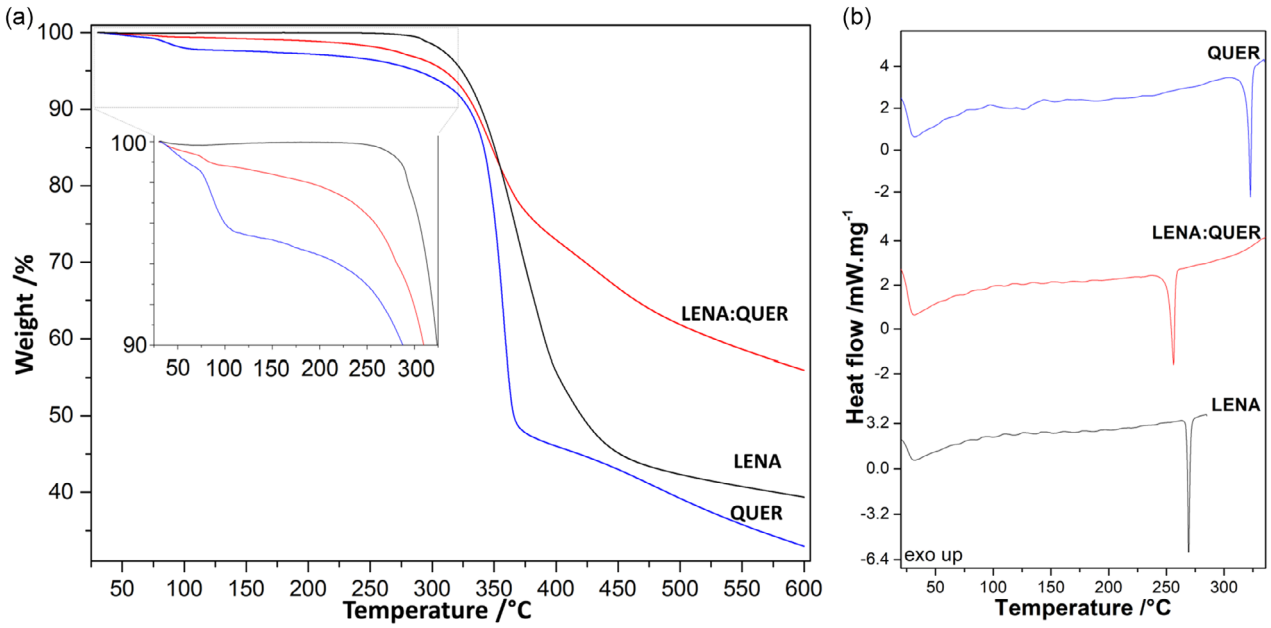

FIGURE 6 | (a) TGA curves in N_2 atmosphere of LENA (black curve), QUER (blue curve), and LENA•QUER cocrystal (red curve) performed at 5°C min^{-1} (b) DSC curves in N_2 atmosphere of LENA (black curve), QUER (blue curve), and LENA•QUER cocrystal (red curve) performed at 10°C min^{-1}.

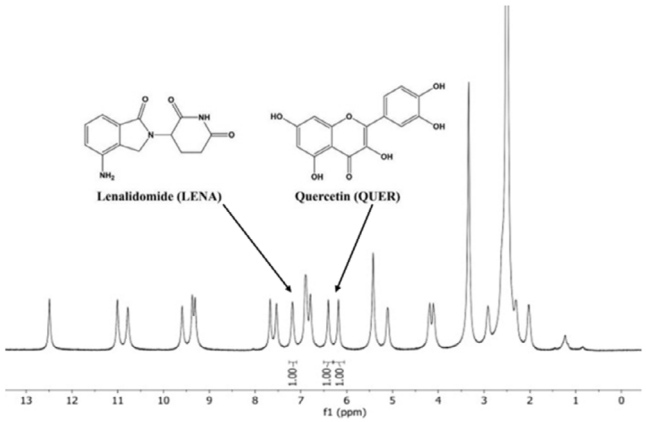

FIGURE 7 | ^{1}H-NMR spectrum in DMSO-d_6 of the LENA•QUER cocrystal, showing the ratio between peaks attributed to LENA and QUER.

components (Figure S12, Supporting Information), the integral of a LENA signal at 7.15 ppm and the two signals of QUER at 6.36 and 6.14 ppm were used to assess the cocrystal formation. As can be seen in Figure 7, the integrals representing the two components are in a 1:1 ratio confirming the ratio.

The solubility data for LENA and the LENA•QUER cocrystal synthesized by slurry, LAG, and RAM methods are shown in Figure 8. LENA alone exhibited a solubility of 5.82 ± 0.63 mg.mL^{-1} at 1 h in pH 1.6, which decreased to 4.51 ± 0.054 mg.mL^{-1} at 24 h. The large standard deviation at the 1 h timepoint and the decline in solubility over time at pH 1.6 suggest a solid-state transformation of LENA into its dihydrate form [30] (Figure S12). In fasted state simulated intestinal fluid (FaSSIF), LENA's solubility was more stable over time, with a 24-hour value of 0.96 ± 0.029 mg.mL^{-1}.

In contrast, the solubility of the cocrystal, regardless of the manufacturing method, was lower than that of pure LENA under both pH conditions tested, and no supersaturation was observed.

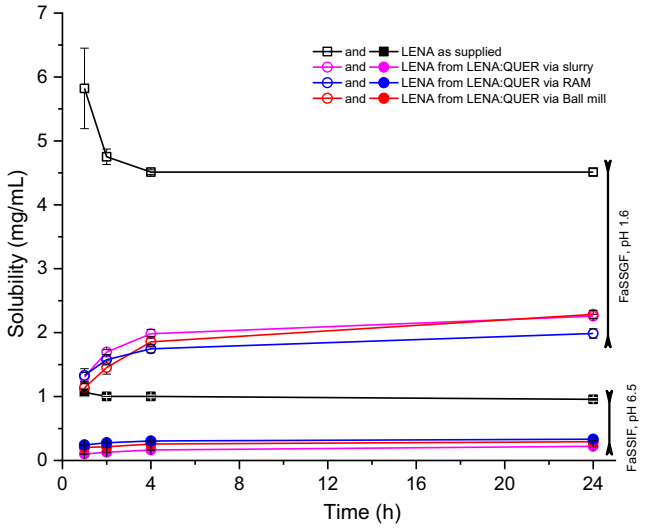

FIGURE 8 | Solubility studies of LENA and LENA•QUER cocrystal synthesized by LAG, RAM, and slurry in FaSSGF (pH = 1.6) and FaSSIF (pH = 6.5).

At the 24-hour timepoint, the solubility of the cocrystal (measured as LENA) at pH 1.6 was 2.26 ± 0.031, 2.29 ± 0.065, and 1.99 ± 0.073 mg.mL^{-1} for the cocrystals produced via slurry, LAG, and RAM, respectively. In FaSSIF, the solubility values were 0.22 ± 0.007, 0.29 ± 0.002, and 0.33 ± 0.023 mg.mL^{-1} for the same respective methods.

A solid-state transformation of the cocrystal to LENA dihydrate was observed under acidic conditions, while the cocrystal structure remained stable during the solubility studies in FaSSIF (Figure S13, Supporting Information).

The results of solubility studies suggest that the cocrystal may function as an extended-release form of LENA, similar to the melamine-based cocrystal described by Screen et al. [46].

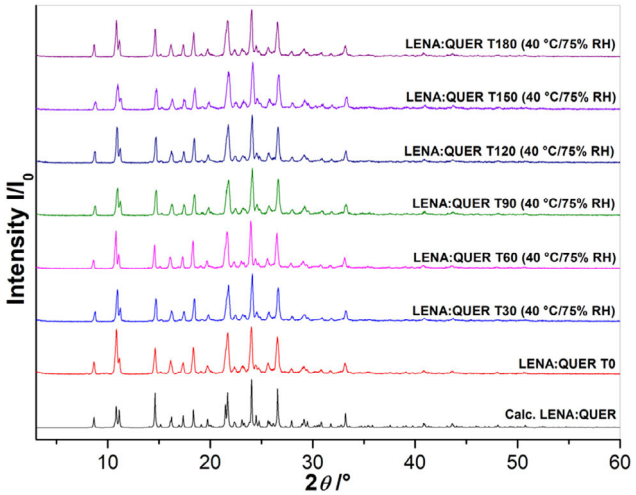

FIGURE 9 | PXRD patterns of LENA and LENA•QUER cocrystal before and after 6 months under accelerated conditions (40°C, 75% R.H.).

2.8 | Accelerated Stability Test

The stability of both LENA and the LENA•QUER cocrystal was monitored under accelerated conditions of 75% of RH at 40°C for 180 days (Figure 9). PXRD analysis revealed that even in extreme humidity conditions, both compounds remained stable without a polymorphic transformation or deliquescence occurring. These results allow us to infer that atmospheric relative humidity does not represent a risk parameter for handling and storage of these compounds in the solid state. In addition, the results showed that this cocrystal is stable for more than 2 years in regions with climatic zones I and II [81].

3 | Conclusion

In this work, crystal engineering strategies were used to design a new LENA•QUER cocrystal. This cocrystal was successfully achieved by different mechanochemical and solution approaches, including LAG in a ball-mill, LA-RAM, slurry, and slow evaporation. Comparing the amount of solvent used in each approach and the total time of synthesis of this cocrystal, mechanochemical process is highlighted for spending less solvent and lower time of synthesis compared to solution and slow evaporation, being a faster route to obtain this cocrystal. Supramolecular synthon analysis shows that the cocrystal structure is stabilized especially through $O–H_{QUER}\cdots O_{LENA}$/$O–H_{QUER}\cdots N_{LENA}$/$N–H_{LENA}\cdots O_{QUER}$ hydrogen bonds. Thermal analysis reveals that this cocrystal has a lower melting point compared with the starting materials. Solubility studies showed that the cocrystal remains stable without solid-state transformation in FaSSIF conditions. Regardless of the synthetic method, LENA•QUER cocrystal has lower solubility compared with pure LENA, suggesting that the cocrystal may function as an extended-release form of LENA. This study provides valuable insights into the design and development of cocrystals using different synthetic routes, in which both mechanochemical approaches have been shown to deliver the desired product faster and using much less amount of solvent, intending to modify the physicochemical properties to improve the way of administration of this drug.

Acknowledgments

V.A., M.T.D, and A.C.S.C. acknowledge funding fromFundação para a Ciência e Tecnologia, and Ministério da Ciência, Tecnologia e Ensino Superior (FCT, Portugal) for the CQE projects UID/00100/2025 (https://doi.org/10.54499/UID/00100/2025); UID/PRR/00100/2025 (https://doi.org/10.54499/UID/PRR/00100/2025); UID/PRR2/00100/2025 (https://doi.org/10.54499/UID/PRR2/00100/2025), and IMS project LA/P/0056/2020 (https://doi.org/10.54499/LA/P/0056/2020). M.S. acknowledges FCT/MCTES for the project UID/50006-Laboratório Associado para a Química Verde- Tecnologias e Processos Limpos, and the Individual Call to Scientific Employment Stimulus 2022 (https://doi.org/10.54499/2022.01388.CEECIND/CP1724/CT0003). C.B.G. acknowledges FCT/MCTES for the LAQV-REQUIMTE projects UID/50006/2025, UID/PRR/50006/2025 and LA/P/0008/2020 (https://doi.org/10.54499/UID/50006/2025, https://doi.org/10.54499/UID/PRR/50006/2025 and https://doi.org/10.54499/LA/P/0008/2020). V.A. and C.B.G. further acknowledge the Scientific Employment Stimulus- FCT-Tenure for funding, as well as Plano de Recuperação e Resiliência (PRR) n.º 02/C06i06/2024 (2023.15700.TENURE.042 and 2023.11076.TENURE.117).

Funding

Funded by the European Union. Views and opinions expressed are however those of the author(s) only and do not necessarily reflect those of the European Union or HaDEA. Neither the European Union nor the granting authority can be held responsible for them. The authors acknowledge IMPACTIVE (Innovative Mechanochemical Processes to synthesize green ACTIVE pharmaceutical ingredients) [82, 83]. The research project funded from the European Union's Horizon Europe research and innovation programme (European Health and Digital Executive Agency) under grant agreement No. 101057286, Fundação para a Ciência e a Tecnologia (Grants UID/00100/2025, LA/P/0056/2020, UID/50006, CEECIND/CP1724/CT0003, UID/50006/2023, LA/P/0008/2020, 2023.15700.TENURE.042, 2023.11076.TENURE.117).

Conflicts of Interest

The authors declare no conflicts of interest.

Data Availability Statement

The data that support the findings of this study are available from the corresponding author upon reasonable request.

References

1. I. R. Speight, K. J. Ardila-Fierro, J. G. Hernández, et al., "Ball Milling for Mechanochemical Reactions," *Nature Reviews Methods Primers* 5, no. 29 (2025): 1–18.

2. M. Mureşan-Pop, S. Simon, E. Bodoki, et al., "Mechanochemical Synthesis of New Praziquantel Cocrystals: Solid-State Characterization and Solubility," *Crystal Growth & Design* 24 (2024): 4668–4681.

3. J. L. Do and T. Friščić, "Mechanochemistry: A Force of Synthesis," *ACS Central Science* 3 (2017): 13–19.

4. A. Nari, J. S. Ovens, and D. L. Bryce, "Halogen-Bonded Cocrystals *via* Resonant Acoustic Mixing," *RSC Mechanochemistry* 1 (2024): 50–62.

5. T. Friščić, C. Mottillo, and H. M. Titi, "Mechanochemistry for Synthesis," *Angewandte Chemie International Edition* 59 (2020): 1018–1029.

6. L. Gonnet, C. B. Lennox, J. L. Do, et al., "Metal-Catalyzed Organic Reactions by Resonant Acoustic Mixing," *Angewandte Chemie International Edition* 61 (2022): e202115030.

7. F. Cuccu, L. De Luca, F. Delogu, et al., "Mechanochemistry: New Tools to Navigate the Uncharted Territory of "Impossible" Reactions," *ChemSusChem* 15 (2022): e202200362.

8. T. Auvray and T. Friščić, "Shaking Things From the Ground-Up: A Systematic Overview of the Mechanochemistry of Hard and High-Melting Inorganic Materials," *Molecules* 28 (2023): 897.

9. T. Friščić, S. L. Childs, S. A. A. Rizvi, and W. Jones, "The Role of Solvent in Mechanochemical and Sonochemical Cocrystal Formation: A Solubility-Based Approach for Predicting Cocrystallisation Outcome," *CrystEngComm* 11 (2009): 418–426.

10. Y. Xiao, C. Wu, X. Hu, et al., "Mechanochemical Synthesis of Cocrystal: From Mechanism to Application," *Crystal Growth & Design* 23 (2023): 4680–4700.

11. V. Štrukil, "Mechanochemical Organic Synthesis: The Art of Making Chemistry Green," *Synlett* 29 (2018): 1281–1288.

12. A. Mukherjee, R. D. Rogers, and A. S. Myerson, "Cocrystal Formation by Ionic Liquid-Assisted Grinding: Case Study with Cocrystals of Caffeine," *CrystEngComm* 20 (2018): 3817–3821.

13. D. Hasa, G. Schneider, D. Voinovich, and W. Jones, "Cocrystal Formation through Mechanochemistry: From Neat and Liquid-Assisted Grinding to Polymer-Assisted Grinding," *Angewandte Chemie International Edition* 54 (2015): 7371–7375.

14. A. A. L. Michalchuk and T. Friščić, "Moving Mechanochemistry Forward: Mechanochemistry and the Non-covalent Bond," *RSC Mechanochem* 2 (2025): 333–335.

15. G. R. Desiraju and G. W. Parshall, *Crystal Engineering: The Design of Organic Solids* (Elsevier, 1989).

16. G. R. Desiraju, "Crystal Engineering: From Molecule to Crystal," *Journal of the American Chemical Society* 135 (2013): 9952–9967.

17. D. J. Berry and J. W. Steed, "Pharmaceutical Cocrystals, Salts and Multicomponent Systems; Intermolecular Interactions and Property Based Design," *Advanced Drug Delivery Reviews* 117 (2017): 3–24.

18. G. Bolla, B. Sarma, and A. K. Nangia, "Crystal Engineering of Pharmaceutical Cocrystals in the Discovery and Development of Improved Drugs," *Chemical Reviews* 122 (2022): 11514–11603.

19. C. B. Aakeröy, N. R. Champness, and C. Janiak, "Recent Advances in Crystal Engineering," *CrystEngComm* 12 (2010): 22–43.

20. R. Pepinsky, "Crystal Engineering—New Concept in Crystallography," *The Physical Review* 100 (1955): 971.

21. G. M. J. Schmidt, "Photodimerization in the Solid State," *Pure and Applied Chemistry* 27 (1971): 647–678.

22. N. K. Duggirala, M. L. Perry, Ö. Almarsson, and M. J. Zaworotko, "Pharmaceutical Cocrystals: Along the Path to Improved Medicines," *Chemical Communications* 52 (2016): 640–655.

23. G. Liu, H. Li, R. Gou, and C. Zhang, "Packing Structures of CL-20-Based Cocrystals," *Crystal Growth & Design* 18 (2018): 7065–7078.

24. I. P. Veronez, J. S. P. Daniel, C. E. C. Júnior, J. S. Garcia, and M. G. Trevisan, "Development, Characterization, and Stability Studies of Ethinyl Estradiol Solid Dispersion," *Journal of Thermal Analysis and Calorimetry* 120 (2015): 573–581.

25. R. Thakuria, A. Delori, W. Jones, M. P. Lipert, L. Roy, and N. Rodríguez-Hornedo, "Pharmaceutical Cocrystals and Poorly Soluble Drugs," *International Journal of Pharmaceutics* 453 (2013): 101–125.

26. D. Tan and F. García, "Main Group Mechanochemistry: From Curiosity to Established Protocols," *Chemical Society Reviews* 48 (2019): 2274–2292.

27. T. Friščić and W. Jones, "Benefits of Cocrystallisation in Pharmaceutical Materials Science: an Update," *The Journal of Pharmacy and Pharmacology* 62 (2010): 1547–1559.

28. F. Fontana, P. Figueiredo, P. Zhang, J. T. Hirvonen, D. Liu, and H. A. Santos, "Production of Pure Drug Nanocrystals and Nano Co-Crystals by Confinement Methods," *Advanced Drug Delivery Reviews* 131 (2018): 3–21.

29. S. Aitipamula, R. Banerjee, A. K. Bansal, et al., "Polymorphs, Salts, and Cocrystals: What's in a Name?," *Crystal Growth & Design* 12 (2012): 2147–2152.

30. J. X. Song, Y. Yan, J. Yao, J. M. Chen, and T. B. Lu, "Improving the Solubility of Lenalidomide via Cocrystals," *Crystal Growth & Design* 14 (2014): 3069–3077.

31. Ö. Almarsson and M. J. Zaworotko, "Crystal Engineering of the Composition of Pharmaceutical Phases. Do Pharmaceutical Co-Crystals Represent a New Path to Improved Medicines?," *Chemical Communications* no. 17 (2004): 1889–1896.

32. G. R. Desiraju, "Supramolecular Synthons in Crystal Engineering—A New Organic Synthesis," *Angewandte Chemie International Edition in English* 34 (1995): 2311–2327.

33. M. M. Haskins, M. Lusi, and M. J. Zaworotko, "Supramolecular Synthon Promiscuity in Phosphoric Acid–Dihydrogen Phosphate Ionic Cocrystals," *Crystal Growth & Design* 22 (2022): 3333–3342.

34. T. K. Adalder, R. Sankolli, and P. Dastidar, "Homo- or Heterosynthon? A Crystallographic Study on a Series of New Cocrystals Derived From Pyrazinecarboxamide and Various Carboxylic Acids Equipped with Additional Hydrogen Bonding Sites," *Crystal Growth & Design* 12 (2012): 2533–2542.

35. M. L. Cheney, D. R. Weyna, N. Shan, M. Hanna, L. Wojtas, and M. J. Zaworotko, "Coformer Selection in Pharmaceutical Cocrystal Development: A Case Study of a Meloxicam Aspirin Cocrystal That Exhibits Enhanced Solubility and Pharmacokinetics," *Journal of Pharmaceutical Sciences* 100 (2011): 2172–2181.

36. M. Khalaji, M. J. Potrzebowski, and M. K. Dudek, "Virtual Cocrystal Screening Methods as Tools to Understand the Formation of Pharmaceutical Cocrystals—A Case Study of Linezolid, a Wide-Range Antibacterial Drug," *Crystal Growth & Design* 21 (2021): 2301–2314.

37. L. Fábián, "Cambridge Structural Database Analysis of Molecular Complementarity in Cocrystals," *Crystal Growth & Design* 9 (2009): 1436–1443.

38. C. R. Groom, I. J. Bruno, M. P. Lightfoot, and S. C. Ward, "The Cambridge Structural Database," *Acta Crystallographica Section B Structural Science, Crystal Engineering and Materials* 72 (2016): 171–179.

39. M. Karimi-Jafari, L. Padrela, G. M. Walker, and D. M. Croker, "Creating Cocrystals: A Review of Pharmaceutical Cocrystal Preparation Routes and Applications," *Crystal Growth & Design* 18 (2018): 6370–6387.

40. M. Guo, X. Sun, J. Chen, and T. Cai, "Pharmaceutical Cocrystals: A Review of Preparations, Physicochemical Properties and Applications," *Acta Pharmaceutica Sinica B* 11 (2021): 2537–2564.

41. D. D. Kara and M. Rathnanand, "Cocrystals and Drug–Drug Cocrystals of Anticancer Drugs: A Perception towards Screening Techniques, Preparation, and Enhancement of Drug Properties," *Crystals* 12 (2022): 1337.

42. P. S. Panzade, G. R. Shendarkar, and D. A. Kulkarni, "Hot Melt Extrusion: an Emerging Green Technique for the Synthesis of High-Quality Pharmaceutical Cocrystals," *Journal of Pharmaceutical Innovation* 17 (2022): 283–293.

43. K. Nagapudi, E. Y. Umanzor, and C. Masui, "High-Throughput Screening and Scale-up of Cocrystals Using Resonant Acoustic Mixing," *International Journal of Pharmaceutics* 521 (2017): 337–345.

44. A. Bodach, A. Portet, F. Winkelmann, et al., "Scalability of Pharmaceutical Co-Crystal Formation by Mechanochemistry in Batch," *ChemSusChem* 17 (2024): e202301220.

45. Y. Zhuo, Y. G. Zhao, and Y. Zhang, "Enhancing Drug Solubility, Bioavailability, and Targeted Therapeutic Applications through Magnetic Nanoparticles," *Molecules* 29 (2024): 1–35.

46. M. A. Screen, G. Tomkinson, J. F. McCabe, et al., "Designing Lenalidomide Cocrystals with an Extended-Release Profile for Improved Pulmonary Drug Delivery," *New Journal of Chemistry* 2 (2025): 6535–6543.

47. Z. Yang, D. Shao, and G. Zhou, "Solubility Parameter of Lenalidomide for Predicting the Type of Solubility Profile and Application of Thermodynamic Model," *The Journal of Chemical Thermodynamics* 132 (2019): 268–275.

48. J. X. Song, J. M. Chen, and T. B. Lu, "Lenalidomide–Gallic Acid Cocrystals with Constant High Solubility," *Crystal Growth & Design* 15 (2015): 4869–4875.

49. K. Ravikumar and B. Sridhar, "Lenalidomide, an Antineoplastic Drug, and Its Hemihydrate," *Acta Crystallographica Section C Crystal Structure Communications* 65 (2009): o502–505.

50. R. Chennuru, P. Muthudoss, R. S. Voguri, et al., "Iso-Structurality Induced Solid Phase Transformations: A Case Study with Lenalidomide," *Crystal Growth & Design* 17 (2017): 612–628.

51. Q. Zhang, Y. Zhu, Y. Xu, H. Yang, W. Li, and X. Zhang, "Different Thermal and Solubility Properties with an Identical Crystal Structure – Case of Lenalidomide Hydrate," *CrystEngComm* 27 (2025): 2815–2823.

52. G. A. Valdivia-Berroeta, K. Sarpal, and N. C. Gonnella, "OPTICS: Operant Probability Theory in Crystal Solutions, Application of ssNMR, and Probability Theory in Polymorph Identification," *Crystal Growth & Design* 21 (2021): 5904–5913.

53. X. Chen, D. Li, J. Wang, Z. Deng, and H. Zhang, "Lenalidomide Acesulfamate: Crystal Structure, Solid State Characterization and Dissolution Performance," *Journal of Molecular Structure* 1175 (2019): 852–857.

54. J. S. Patton and P. R. Byron, "Inhaling Medicines: Delivering Drugs to the Body through the Lungs," *Nature Reviews Drug Discovery* 6 (2007): 67–74.

55. N. Chen, S. Zhou, and M. Palmisano, "Clinical Pharmacokinetics and Pharmacodynamics of Lenalidomide," *Clinical Pharmacokinetics* 56 (2017): 139–152.

56. S. A. Mir, A. Dar, L. Hamid, et al., "Flavonoids as Promising Molecules in the Cancer Therapy: An Insight," *Current Research in Pharmacology and Drug Discovery* 6 (2024): 100167.

57. H. S. Tuli, V. K. Garg, S. Bhushan, et al., "Natural Flavonoids Exhibit Potent Anticancer Activity by Targeting microRNAs in Cancer: A Signature Step Hinting towards Clinical Perfection," *Translational Oncology* 27 (2023): 101596.

58. A. Murakami, H. Ashida, and J. Terao, "Multitargeted Cancer Prevention by Quercetin," *Cancer Letters* 269 (2008): 315–325.

59. X. Wang, Y. Yang, Y. An, and G. Fang, "The Mechanism of Anticancer Action and Potential Clinical use of Kaempferol in the Treatment of Breast Cancer," *Biomedicine & Pharmacotherapy* 117 (2019): 109086.

60. U. B. R. Khandavilli, E. Skořepová, A. S. Sinha, et al., "Cocrystals and a Salt of the Bioactive Flavonoid: Naringenin," *Crystal Growth & Design* 18 (2018): 4571–4577.

61. M. Elshaer, S. K. Osman, A. M. Mohammed, and G. Zayed, "Co-crystallization of Hesperidin with different co-formers to enhance solubility, antioxidant and anti-inflammatory activities," *Pharmaceutical Development and Technology* 29 (2024): 1–12.

62. D. J. Timmons, M. R. Pacheco, K. A. Fricke, and C. Slebodnick, "Assembling Extended Structures with Flavonoids," *Crystal Growth & Design* 8 (2008): 2765–2769.

63. C. Duan, Y. Chen, Y. Zhang, et al., "Two Cocrystals of Olaparib with Flavonoids toward Sustained Release: Structure, Dissolution Behavior, and Anticancer Activity Analysis," *Crystal Growth & Design* 22 (2022): 4885–4894.

64. C. C. Lee, J. Hee Lim, A. Young Cho, et al., "Molecular Structures of Flavonoid Co-Formers for Cocrystallization with Carbamazepine," *Journal of Industrial and Engineering Chemistry* 118 (2023): 309–317.

65. A. Alvani and A. Shayanfar, "Cocrystallization for Improving Anticancer Activity of Drugs," *Crystal Research and Technology* 59 (2024): 2300253.

66. H. M. Yin, J. Y. Xie, J. Y. Jiang, et al., "Strategy to Tune the Performance of Two Drug Components: Drug–Drug Cocrystals of Lobaplatin with Flavonoids," *Crystal Growth & Design* 22 (2022): 2602–2610.

67. S. Andres, S. Pevny, R. Ziegenhagen, et al., "Safety Aspects of the Use of Quercetin as a Dietary Supplement," *Molecular Nutrition & Food Research* 62 (2018): 1–15.

68. M. M. Haskins, O. N. Kavanagh, R. Sanii, et al., "Tuning the Pharmacokinetic Performance of Quercetin by Cocrystallization," *Crystal Growth & Design* 23 (2023): 6059–6066.

69. K. Teshima, R. Asasutjarit, and S. Theeramunkong, "Cocrystal Formation of Quercetin and Nutraceutical Coformers via a Facile Technique with Improved Solubility and Biological Properties," *ACS Omega* 11, no. 4 (2026): 5973–5982.

70. L. Wang, S. Li, X. Xu, et al., "Drug-Drug Cocrystals of Theophylline with Quercetin," *Journal of Drug Delivery Science and Technology* 70 (2022): 103228.

71. W. Lv, H. Zhang, N. Sai, et al., "The Impact of Quercetin- Geniposide Interaction on the Growth and Properties of Quercetin Nanocrystals," *Natural Product Communications* 20 (2025): 1–14.

72. A. J. Smith, P. Kavuru, L. Wojtas, M. J. Zaworotko, and R. D. Shytle, "Cocrystals of Quercetin with Improved Solubility and Oral Bioavailability," *Molecular Pharmaceutics* 8 (2011): 1867–1876.

73. M. Özsoy, Y. P. Tok, G. G. Eskiler, et al., "The Lenalidomide Derivative Loaded and Quercetin Modified MIL-100 Based Novel Drug Delivery System for Breast Cancer Treatment," *Journal of Drug Delivery Science and Technology* 108 (2025): 106923.

74. R. Jayachandiran, S. J. Akkarapakam, and K. Thangavel, "Virtual Screening of Pharmaceutical Cocrystals Using Machine Learning Algorithms," *Crystal Growth & Design* 25 (2025): 3100–3109.

75. M. C. Etter, "Encoding and Decoding Hydrogen-Bond Patterns of Organic Compounds," *Accounts of Chemical Research*. (1990): 120–126.

76. S. Pagola, "Outstanding Advantages, Current Drawbacks, and Significant Recent Developments in Mechanochemistry: A Perspective View," *Crystals* 13 (2023): 1–33.

77. P. R. Spackman, M. J. Turner, J. J. McKinnon, et al., "*CrystalExplorer* : A Program for Hirshfeld Surface Analysis, Visualization and Quantitative Analysis of Molecular Crystals," *Journal of Applied Crystallography* 54 (2021): 1006–1011.

78. J. Karuppasamy, A. Zochedh, A. Shunmuganarayanan, and A. B. Sultan, "Solid State Synthesis of Zwitterionic Cocrystal 5-Fluorouracil L-Phenylalanine Explicated via Structural, Spectroscopy, Quantum Chemicals, Hirshfeld and Docking Analysis," *Journal of Molecular Structure* 1302 (2024): 137386.

79. L. Wang, Y. Yan, X. Zhang, and X. Zhou, "Novel Pharmaceutical Cocrystal of Lenalidomide with Nicotinamide: Structural Design, Evaluation, and Thermal Phase Transition Study," *International Journal of Pharmaceutics* 613 (2022): 121394.

80. D. L. Pavia, G. M. Lampman, G. S. Kriz, and J. R. Vyvyan, *Introduction to Spectroscopy* (Brooks/Cole, 2009).

81. W. Grimm, "Extension of the International Conference on Harmonization Tripartite Guideline for Stability Testing of New Drug Substances and Products to Countries of Climatic Zones III and IV," *Drug Development and Industrial Pharmacy* 24 (2008): 313–325.

82. "*IMPACTIVE: Innovative Mechanochemical Processes to synthesize green ACTIVE pharmaceutical ingredients*," 2026, "https://mechanochemistry.eu/.

83. J. J. Sáenz de la Torre, L. Flamarique, F. Gomollon-Bel, and E. Colacino, "Mechanochemistry in Europe: where We Come From and where We Are now," *Open Research Europe* 5 (2025): 73.

Supporting Information

Additional supporting information can be found online in the Supporting Information section. The Supporting Information is available free of charge. PXRD, thermal analyses, tables and additional figures (PDF). Accession Codes CCDC 2445699, contain the supplementary crystallographic data for this paper. These data can be obtained free of charge via www.ccdc.cam.ac.uk/data_request/ cif, or by emailing data_request@ccdc.cam.ac.uk, or by contacting The Cambridge Crystallographic Data Centre, 12 Union Road, Cambridge CB2 1EZ, UK; fax: +44 1223 336033.